

TABLE OF CONTENTS

	Page
Acknowledgements	iii
Abstract (English)	v
Abstract (Thai)	vii
Table of Contents	ix
List of Tables	xiv
List of Figures	xviii
Abbreviations and Symbols	xxii
Chapter 1 Introduction	
1.1 Statement of problems	1
1.2 Literature reviews	3
1.2.1 Background and related studies	3
1.2.1.1 <i>Terminalia chebula</i> Retzius	3
1.2.1.2 <i>Terminalia bellerica</i>	7
1.2.1.3 <i>Etilingera elatior</i> (Jack) R.M. Smith	9
1.2.1.4 <i>Rosa damascena</i>	12
1.2.1.5 <i>Rafflesia kerrii</i> Meijer	14
1.2.2 Phenolic compounds	17
1.2.3 Cytotoxicity assay	18
1.2.3.1 MTT assay	18
1.2.3.2 XTT assay	19

TABLE OF CONTENTS (continued)

	Page
1.2.3.3 Sulforhodamine B (SRB) assay	20
1.2.3.4 Dye exclusion assay	21
1.2.3.5 Dye inclusion assay	21
1.2.4. Mutagenicity assay by Ames test	22
1.2.5 Antimutagenicity assay	23
1.2.6 Tyrosinase activity in melanogenesis mechanism	25
1.2.7 Morphological changes of UV treated cell lines	27
1.3 Research Objectives	28
Chapter 2 Materials and Methods	
2.1 Materials	29
2.1.1 Chemicals	29
2.1.2 Instruments	31
2.1.3 Microorganisms	32
2.1.4 Cell cultures	33
2.1.5 Plant Extracts	34
2.2 Methods	34
2.2.1 Preparation of the plant extracts	34
2.2.2 Characterization of plant extracts	35
2.2.3 Determination of total phenolic content by using Folin-Ciocalteu method	35
2.2.4 Cytotoxicity assay	35

TABLE OF CONTENTS (continued)

	Page
2.2.4.1 Cytotoxicity of the plant extracts in mouse fibroblast cell lines by MTT assay	35
2.2.4.2 Cytotoxicity of the plant extracts in mouse fibroblast cell lines by Dye exclusion method	37
2.2.5 Genotoxicity assay	37
2.2.6 Antimutagenicity assay	39
2.2.7 Investigation of antityrosinase activities in plant extracts	40
2.2.8 Determination of UVA induced morphological changes	41
2.2.9 Determination of UVB induced morphological changes	42
Chapter 3 Results	
3.1 Physical properties of the plant extracts	43
3.2 Characterization of plant extracts by Spectroscopy	44
3.2.1 Characterization of plant extracts by Ultraviolet-visible spectrophotometer (UV-visible spectrophotometer)	45
3.2.2 Characterization of plant extracts by Infrared spectroscopy (IR)	48
3.2.3 Characterization of plant extracts by nuclear magnetic resonance (NMR)	56
3.3 Determination of total phenolic content in plant extracts	61
3.4 Cytotoxicity of the plant extracts	63
3.4.1 Cytotoxicity of the plant extracts in normal and melanoma mouse fibroblast cell lines using MTT assay	63

TABLE OF CONTENTS (continued)

	Page
3.4.2 Cytotoxicity of the plant extracts in normal and melanoma mouse fibroblast cell lines by Dye exclusion method	65
3.5 Mutagenicity of plant extracts	67
3.6 Antimutagenicity of plant extracts	73
3.7 Antityrosinase activity of the plant extracts	88
3.8 Morphological changes of normal and melanoma mouse fibroblast cell lines after induced by UVA radiation	90
3.9 Morphological changes of normal and melanoma mouse fibroblast cell lines after induced by UVB radiation	102
Chapter 4 Discussions & Conclusions	
4.1 Discussions	112
4.2 Conclusions	123
References	126
Appendices	139
Appendix A	140
Appendix B	146
Appendix C	163
Appendix D	171
Appendix E	173
Appendix F	175
Appendix G	177

TABLE OF CONTENTS (continued)

	Page
Appendix H	178
Appendix I	188
Curriculum vitae	190



ลิขสิทธิ์มหาวิทยาลัยเชียงใหม่
 Copyright© by Chiang Mai University
 All rights reserved

TABLE OF TABLES

Table	Page
1.1 The genotype of the <i>Samonella</i> strains which were used in Ames test	23
2.1 Genotypes of the mutant bacterial <i>S. typhimurium</i> strains TA98 and TA100	33
2.2 List of plants, parts and solvent used for study	34
3.1 Physical appearance of the plant extracts	44
3.2 The total phenolic content (TPCs) of the five plant extracts after examined by Folin-Ciocalteu method	62
3.3 Cytotoxicity of plant extracts on normal mouse fibroblast L929 and melanoma fibroblast B16F10 cell lines expressed as 50% cytotoxicity dose (CD ₅₀) values which were obtained in MTT assay for 48 h	64
3.4 Cytotoxicity of plant extracts on normal mouse fibroblast L929 and melanoma fibroblast B16F10 cell lines expressed as 50% cytotoxicity dose (CD ₅₀) values which were obtained in dye exclusion for 24 h	66
3.5 Mutagenicity of 70% hydroglycol extract of <i>T. chebula</i> Retz. at concentrations between 0.088 and 87.34 mg/0.1 ml in <i>S. typhimurium</i> TA98 and TA100 strains	68
3.6 Mutagenicity of 70% hydroglycol extract of <i>T. bellerica</i> at concentrations between 0.088 and 87.34 mg/0.1 ml in <i>S. typhimurium</i> TA98 and TA100 strains	69

TABLE OF TABLES (continued)

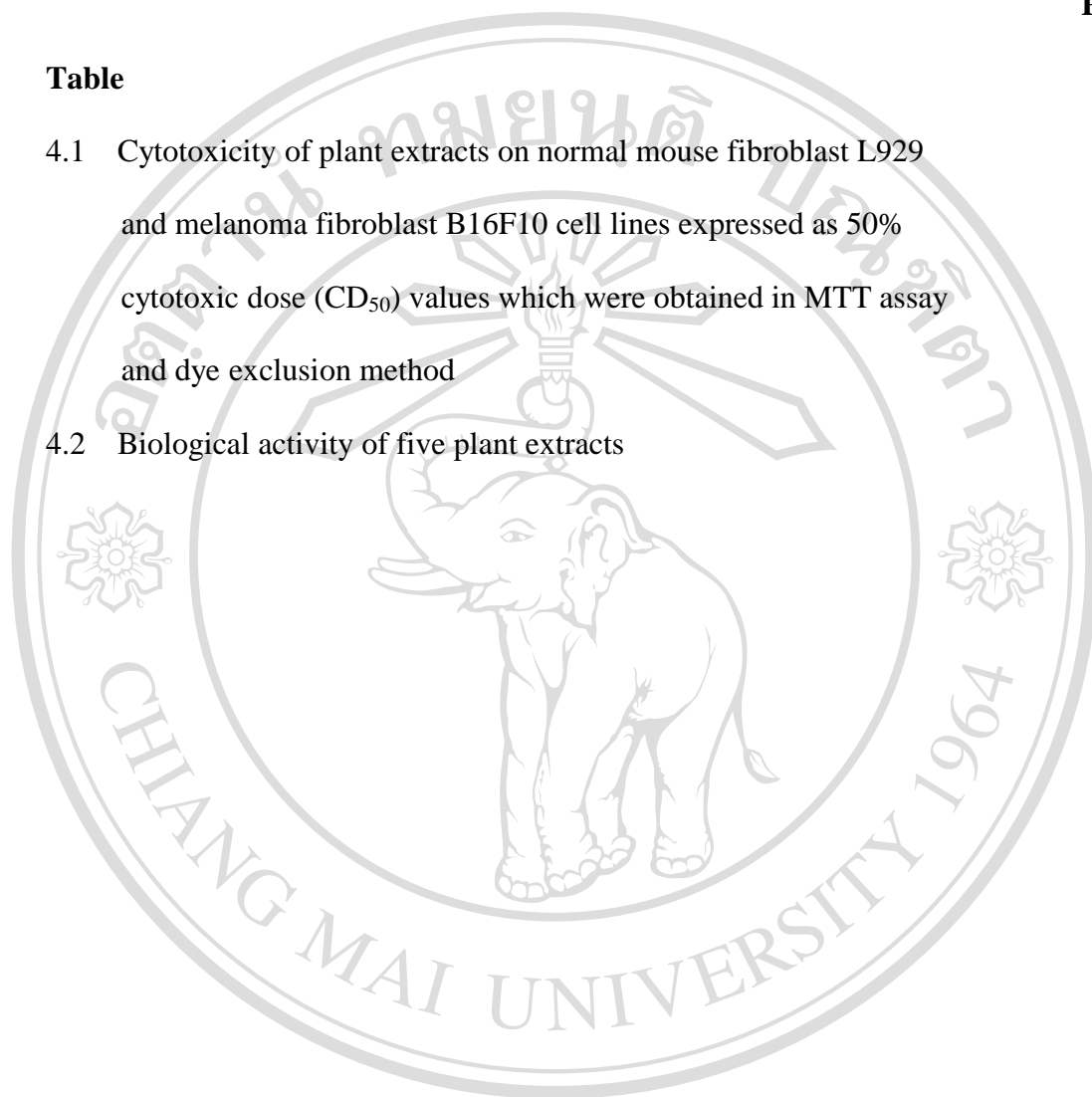
Table	Page
3.7 Mutagenicity of 50% hydroglycol extract of <i>E. elatior</i> (Jack) R.M. Smith at concentrations between 0.088 and 87.34 mg/0.1 ml in <i>S. typhimurium</i> TA98 and TA100 strains	70
3.8 Mutagenicity of 50% hydroglycol extract of <i>R. damascena</i> at concentrations between 0.088 and 87.34 mg/0.1 ml in <i>S. typhimurium</i> TA98 and TA100 strains	71
3.9 Mutagenicity of 50% hydroglycol extract of <i>R. kerrii</i> Meijer at concentrations between 0.088 and 87.34 mg/0.1 ml in <i>S. typhimurium</i> TA98 and TA100 strains	72
3.10 Inhibition of mutagenicity by <i>T. chebula</i> Retz. in <i>S. typhimurium</i> TA98 assay system	74
3.11 Inhibition of mutagenicity by <i>T. chebula</i> Retz. in <i>S. typhimurium</i> TA100 assay system	75
3.12 Inhibition of mutagenicity by <i>T. bellerica</i> in <i>S. typhimurium</i> TA98 assay system	76
3.13 Inhibition of mutagenicity by <i>T. bellerica</i> in <i>S. typhimurium</i> TA100 assay system	77
3.14 Inhibition of mutagenicity by <i>E. elatior</i> (Jack) R.M. Smith in <i>S. typhimurium</i> TA98 assay system	79
3.15 Inhibition of mutagenicity by <i>E. elatior</i> (Jack) R.M. Smith in <i>S. typhimurium</i> TA100 assay system	80

TABLE OF TABLES (continued)

Table	Page
3.16 Inhibition of mutagenicity by <i>R. damascena</i> in <i>S. typhimurium</i> TA98 assay system	81
3.17 Inhibition of mutagenicity by <i>R. damascena</i> in <i>S. typhimurium</i> TA100 assay system	82
3.18 Inhibition of mutagenicity by <i>R. kerrii</i> Meijer in <i>S. typhimurium</i> TA98 assay system	83
3.19 Inhibition of mutagenicity by <i>R. kerrii</i> Meijer in <i>S. typhimurium</i> TA100 assay system	84
3.20 50% inhibition of mutagenicity (IC ₅₀) by five plant extracts on both <i>S. typhimurium</i> strains in presence of metabolic activation	87
3.21 50% inhibition of mutagenicity (IC ₅₀) by five plant extracts on both <i>S. typhimurium</i> strains in absence of metabolic activation	87
3.22 Tyrosinase inhibitory activity of the five plant extracts on mushroom tyrosinase	89
3.23 The morphological changes of normal mouse fibroblast L929 and mouse melanoma B16F10 cell lines after exposed to UVA and treated with the five plant extracts at different concentration	101
3.24 The morphological changes of normal mouse fibroblast L929 and mouse melanoma B16F10 cell lines after exposed to UVA and treated with the five plant extracts at different concentration	111

TABLE OF TABLES (continued)

Table	Page
4.1 Cytotoxicity of plant extracts on normal mouse fibroblast L929 and melanoma fibroblast B16F10 cell lines expressed as 50% cytotoxic dose (CD ₅₀) values which were obtained in MTT assay and dye exclusion method	116
4.2 Biological activity of five plant extracts	125



ลิขสิทธิ์มหาวิทยาลัยเชียงใหม่
 Copyright© by Chiang Mai University
 All rights reserved

TABLE OF FIGURES

Figure	Page
1.1 The fruit of <i>Terminalia chebula</i> Retzius	3
1.2 Chemical structure of chebulagic acid	5
1.3 Chemical structure of 1,2,3,4,6-penta- <i>O</i> -galloyl- β -D-glucose (PGG)	6
1.4 The fruit of <i>Terminalia bellerica</i>	7
1.5 Chemical structure of cannogenol 3- <i>O</i> - β -D-galactopyranosyl-(1 \rightarrow 4)- <i>O</i> - α -L-rhamnopyranoside from the seed of <i>T. bellerica</i>	8
1.6 <i>Etilingera elatior</i> (Jack) R.M. Smith	10
1.7 <i>Rose damascena</i>	13
1.8 <i>Rafflesia kerrii</i> Meijer	15
1.9 Chemical structure of four hydrolysable tannins 1,2,4,6-tetra- <i>O</i> -galloyl- β -D-glucopyranoside, 1,2,6-tri- <i>O</i> -galloyl- β -D-glucopyranoside, 1,4,6-tri- <i>O</i> -galloyl- β -D-glucopyranoside and 1,2,4-tri- <i>O</i> -galloyl- β -D-glucopyranoside and one phenylpropanoid glucoside	16
1.10 Structure of phenol (A), phenolic acid (B), flavonoids (C)	17
1.11 MTT reduction in live cells by mitochondrial reductase results in the Formation of insoluble formazan	19
1.12 Structures of XTT and Formazan	20
1.13 Structure of sulforhodamine B	21
1.14 Eumelanins and pheomelanins biosynthesis pathway	25

TABLE OF FIGURES (continued)

Figure	Page
3.1 Color of the extracts: <i>T. chebula</i> Retz. (MB), <i>T. bellerica</i> (BM), <i>E. elatior</i> (Jack) R.M. Smith (EE), <i>R. damascena</i> (DR) and <i>R. kerrii</i> Meijer (RM)	44
3.2 UV-Visible spectrum of <i>T. chebula</i> Retz. (A), <i>T. bellerica</i> (B), <i>E. elatior</i> (Jack) R.M. Smith (C), <i>R. damascena</i> (D) and <i>R. kerrii</i> Meijer (E) at wavelength between 200 and 500 nm	45
3.3 IR spectrum of <i>T. chebula</i> Retz. (A), <i>T. bellerica</i> (B), <i>E. elatior</i> (Jack) R.M. Smith (C), <i>R. damascena</i> (D) and <i>R. kerrii</i> Meijer (E)	51
3.4 ¹ HNMR spectrum of hydroglycol (A), <i>T. chebula</i> Retz. (B), <i>T. bellerica</i> (C), <i>E. elatior</i> (Jack) R.M. Smith (D), <i>R. damascena</i> (E) and <i>R. kerrii</i> Meijer (F)	58
3.5 Comparison of the total phenolic content of the five plants extracts at mg GAE/g of wet weight which were estimated as gallic acid equivalents	62
3.6 50% cytotoxicity dose (CD ₅₀) of the extracts for mouse normal skin fibroblast L929 and mouse melanoma fibroblast B16F10 cell lines by MTT assay	64
3.7 50% cytotoxicity dose (CD ₅₀) of the extracts for mouse normal skin fibroblast L929 and melanoma skin fibroblast B16F10 cell lines by dye exclusion	66

TABLE OF FIGURES (continued)

Figure	Page
3.8 Antimutagenic activity of five plant extracts in both <i>S. typhimurim</i> after treated with 2-AA and AF-2 in the presence and absence of metabolic activation	85
3.9 Tyrosinase inhibitory activity and 50% inhibitory concentration values of the plant extracts (IC ₅₀) on mushroom tyrosinase	89
3.10 Morphology of normal mouse fibroblast L929 and mouse melanoma B16F10 cell lines after induced by UVA radiation and then treated with <i>T. chebula</i> Retz. extract at the concentration of CD _{3.13} , CD _{6.25} and CD _{12.5}	93
3.11 Morphology of normal mouse fibroblast L929 and mouse melanoma B16F10 cell lines after induced by UVA radiation and treated with <i>T. bellerica</i> extract at the concentrations of CD _{3.13} , CD _{6.25} and CD _{12.5}	94
3.12 Morphology of normal mouse fibroblast L929 and mouse melanoma B16F10 cell lines after induced by UVA radiation and treated with <i>E. elatior</i> (Jack) R.M. Smith extract at the concentrations of CD _{3.13} , CD _{6.25} and CD _{12.5}	97
3.13 Morphology of normal mouse fibroblast L929 and mouse melanoma B16F10 cell lines after induced by UVA radiation and treated with <i>R. damascena</i> extract at the concentrations of CD _{3.13} , CD _{6.25} and CD _{12.5}	98

TABLE OF FIGURES (continued)

Figure	Page
3.14 Morphology of normal mouse fibroblast L929 and mouse melanoma B16F10 cell lines after induced by UVA radiation and treated with <i>R. kerrii</i> Meijer extract at the concentrations of CD _{3.13} , CD _{6.25} and CD _{12.5}	99
3.15 Morphology of normal mouse fibroblast L929 and mouse melanoma B16F10 cell lines after induced by UVB radiation and then treated with <i>T. chebula</i> Retz. extract at the concentration of CD _{3.13} , CD _{6.25} and CD _{12.5}	104
3.16 Morphology of normal mouse fibroblast L929 and mouse melanoma B16F10 cell lines after induced by UVB radiation and treated with <i>T. bellerica</i> extract at the concentrations of CD _{3.13} , CD _{6.25} and CD _{12.5}	105
3.17 Morphology of normal mouse fibroblast L929 and mouse melanoma B16F10 cell lines after induced by UVB radiation and treated with <i>E. elatior</i> (Jack) R.M. Smith extract at the concentrations of CD _{3.13} , CD _{6.25} and CD _{12.5}	107
3.18 Morphology of normal mouse fibroblast L929 and mouse melanoma B16F10 cell lines after induced by UVB radiation and treated with <i>R. damascena</i> extract at the concentrations of CD _{3.13} , CD _{6.25} and CD _{12.5}	108
3.19 Morphology of normal mouse fibroblast L929 and mouse melanoma B16F10 cell lines after induced by UVB radiation and treated with <i>R. kerrii</i> Meijer extract at the concentrations of CD _{3.13} , CD _{6.25} and CD _{12.5}	109

ABBREVIATIONS AND SYMBOLS

°C	degree Celcius
%	percentage
δ	chemical shift (ppm)
μ l	microliter
μ M	micromolar
μ g	microgram
CD ₅₀	50% cytotoxic dose
cm	centimeter
g	gram
GAE	galic acid equivalent
hr	hour
Hz	hertz
IC ₅₀	50% inhibitory concentration
IR	infrared radiation
IU	units of enzyme
J	joule
l	liter
M	molar
mg	milligram
mJ	millijoule
ml	milliliter
min	minute

ลิขสิทธิ์มหาวิทยาลัยเชียงใหม่
 Copyright © by Chiang Mai University
 All rights reserved

mM	millimolar
MTT	3-(4,5-dimethylthiazol-2-yl)-2,5-diphenyltetrazolium bromide
NADH	nicotinamide adenine dinucleotide
NADPH	nicotinamide adenine dinucleotidephosphate
nm	nanometer
NMR	nuclear magnetic resonance
sec	second
SRB	sulforhodamine B
TPC	total phenolic content
UV	Ultraviolet
UV A	Ultraviolet A
UV B	Ultraviolet B
UV C	Ultraviolet C
ν	wave number (cm^{-1})
v/v	volume by volume
V_{max}	maximum initial velocity
W	watt
w/v	weight by volume
XTT	2,3-bis-(2-methoxy-4-nitro-5-sulphophenyl)-2H-tetrazolium-5-carboxanilide

ลิขสิทธิ์มหาวิทยาลัยเชียงใหม่
 Copyright © by Chiang Mai University
 All rights reserved